

# UC Berkeley

## UC Berkeley Previously Published Works

### Title

Crop growth and irrigation interact to influence surface fluxes in a regional climate-cropland model (WRF3.3-CLM4crop)

### Permalink

<https://escholarship.org/uc/item/45f139sp>

### Journal

Climate Dynamics, 45(11-12)

### ISSN

0930-7575

### Authors

Lu, Y

Jin, J

Kueppers, LM

### Publication Date

2015-12-01

### DOI

10.1007/s00382-015-2543-z

Peer reviewed

# Crop growth and irrigation interact to influence surface fluxes in a regional climate-cropland model (WRF3.3-CLM4crop)

Yaqiong Lu · Jiming Jin · Lara M. Kueppers

**Abstract** In this study, we coupled Version 4.0 of the Community Land Model that includes crop growth and management (CLM4crop) into the Weather Research and Forecasting (WRF) model Version 3.3 to better represent interactions between climate and agriculture. We evaluated the performance of the coupled model (WRF3.3-CLM4crop) by comparing simulated crop growth and surface climate to multiple observational datasets across the continental United States. The results showed that although the model with dynamic crop growth overestimated leaf area index (LAI) and growing season length, interannual variability in peak LAI was improved relative to a model with prescribed crop LAI and growth period, which has no environmental sensitivity. Adding irrigation largely improved daily minimum temperature but the RMSE is still higher over irrigated land than non-irrigated land. Improvements in climate variables were limited by an overall model dry bias. However, with addition of an irrigation scheme, soil moisture and surface energy flux partitioning were largely improved at irrigated sites. Irrigation effects were sensitive to crop growth: the

case with prescribed crop growth underestimated irrigation water use and effects on temperature and overestimated soil evaporation relative to the case with dynamic crop growth in moderately irrigated regions. We conclude that studies examining irrigation effects on weather and climate using coupled climate-land surface models should include dynamic crop growth and realistic irrigation schemes to better capture land surface effects in agricultural regions.

**Keywords** WRF · CLM · Dynamic crop growth · Irrigation · Climate · Surface energy flux

## 1 Introduction

The response of agricultural systems to a changing climate has attracted considerable attention due to increased potential for global food crises (Adams et al. 1990; Lawlor and Mitchell 1991; Long et al. 2006; Mendelsohn et al. 1994; Rosenzweig and Parry 1994). Crop models, including both process-based and statistical models, are widely used to simulate space\_\_\_\_\_ climate impacts on crop growth and production. For exam-

spaceY. Lu (✉) · L. M. Kueppers  
Sierra Nevada Research Institute, University of California,  
Merced, Merced, CA, USA e-mail:  
[ylu9@ucmerced.edu](mailto:ylu9@ucmerced.edu)

J. Jin  
Department of Watershed Sciences, Utah State University, Logan, UT, USA

J. Jin  
Department of Plants, Soil, and Climate, Utah State University, Logan, UT, USA

L. M. Kueppers  
Earth Sciences Division, Lawrence Berkeley National Laboratory, Berkeley, CA, USA

spaceple, a warming of 2–4 °C could increase crop development rates, which would shorten the growing season and alter crop phenology calendars (Butterfield and Morison 1992; Peiris et al. 1995); elevated atmospheric CO<sub>2</sub> concentrations can increase crop yield (Brown and Rosenberg 1999; Easterling et al. 1992; Mearns et al. 1992); and yields of wheat, maize, and barley are declining with increased temperature globally (Lobell and Field 2007; Lobell et al. 2008). Although agronomic models have increased our understanding of crop responses to climate change, they have not typically accounted for interactions between climate and crop growth.

Crop growth and climate are highly coupled. Optimum soil temperature and moisture yield the maximum

spaceseed germination rate for a given crop (Covell et al. 1986; Wagenvoort and Bierhuizen 1977). Growing degree days (sum of daily temperature degrees above a baseline) based on the air temperature can be used to predict the phenological phase and physiological activity of crops (Bonhomme 2000). Furthermore, crop productivity is reduced by many forms of environmental stress, such as high temperature, drought, low atmospheric humidity (Lobell et al. 2014), and air pollution (Pessaraki 1999). At the same time, cropland plays a very important biogeophysical role in a changing climate (Feddema et al. 2005; Foley et al. 2005; Pitman et al. 1999). Crops alter the small-scale boundary layer structure (Adegoke et al. 2007), such as surface wind and boundary layer height, with increasing canopy height during the growth processes. Converting forest to cropland generates a higher surface albedo that alters the energy budget (Bonan 2008; Oleson et al. 2004). Cropland also alters water cycles. Both field observations and modeling have shown that conversion of forest to rainfed cropland

can reduce evapotranspiration and precipitation at a regional scale (Sampaio et al. 2007).

Cropland management, such as irrigation, has been found to affect climate through changes in water and energy budgets (Adegoke et al. 2003; Cook et al. 2011; Harding and Snyder 2012b; Jin and Miller 2011; Ozdogan and Salvucci 2004; Sorooshian et al. 2011). Irrigation's impacts on energy budgets are complex. The extra water applied to the soil enhances evapotranspiration, thereby reducing surface temperature through evaporative cooling (Kueppers et al. 2007; Lobell et al. 2009; Sacks et al. 2009). The surface cooling reduces emission of surface long wave radiation, while water vapor in the upper air can absorb and release more long wave radiation to the surface (Boucher et al. 2004; Kueppers and Snyder 2012). Irrigation can also increase net solar radiation at the surface due to the decreased albedo of the wet soil (Otterman 1977). Irrigation increases local and regional precipitation in regions where the atmosphere and soil moisture are highly coupled. For example in the US Great Plains, irrigation enhances convection by increasing convective available potential energy (CAPE) and introduces additional precipitable water, therefore increasing precipitation (DeAngelis et al. 2010; Harding and Snyder 2012a). Although irrigation effects are most significant in irrigated land, irrigation also affects the surrounding region through changes in atmospheric circulation. For example, irrigation affects the Asian summer monsoon by reducing the differential heating between land and sea (Saeed et al. 2009), and irrigation in California's Central Valley strengthens the southwestern US water cycle (Lo and Famiglietti 2013). A key issue is that numerical models used to explore these mechanisms have prescribed crop leaf area values that do not respond to environmental changes or inter-annual variations in weather and climate. This prescribed approach

space could result in significant errors in estimating evapotranspiration from croplands, because crop leaf area and physiological activity are known to dynamically respond to climate variation (Fang et al. 2001; Porter and Semenov 2005). In addition, such an approach cannot be used to predict the effects of future climate on crop processes.

In the past 15 years, several studies have coupled a dynamic crop growth model with a climate model to explore the importance to two-way feedbacks between crop growth and climate. For example, Lu et al. (2001) coupled the daily time step version of the CENTURY model into the Regional Atmospheric Modeling System (RAMS) and found seasonal vegetation phenology strongly influences climate patterns over the central US. Tsvetsinskaya et al. (2001) introduced growth

functions into the Biosphere–Atmosphere Transfer Scheme (BATS) and coupled it into the Atmospheric Research Regional Climate Model (RegCM2) and found up to a 45 % change in surface energy fluxes in response to dynamic leaf area index (LAI). Osborne et al. (2007) coupled a General Large Area Model for annual crops into a global climate model (HadAM3) and found growing season temperature variability was increased by up to 40 % with the inclusion of dynamic crops (Osborne et al. 2009). Levis et al. (2012) incorporated an agriculture version of the Community Land Model (CLM) into the Community Earth System Model (CESM) and found dynamic crop growth not only improves biogeophysical simulations (e.g., surface energy fluxes), but also improves biogeochemistry simulations (e.g., net ecosystem exchange).

These studies revealed that dynamic crop growth strongly influences regional climate patterns by altering land surface energy fluxes. However, except for Levis et al. (2012), none of these studies validated the surface energy fluxes against observations before and after incorporating the dynamic crop growth model. The role of crop growth in regional climate systems has not been quantitatively investigated. Furthermore, the extent to which dynamic crop growth alters irrigation effects on climate is not well known. Only Xu et al. (2005) and Liang et al. (2012) took irrigation into account in their studies, but they were focused mainly on how irrigation affects cotton yields and the irrigation effects on climate after adding a dynamic crop scheme have not been discussed. In addition, as a widely used regional climate model, the Weather Research and Forecasting Model (WRF) does not include a dynamic crop growth model, and is therefore limited in its capability for studying the interactions between climate and crop growth. To fill these gaps, we incorporated a crop growth model and an irrigation scheme into WRF. The objectives of this study were: (1) to evaluate a newly coupled regional climate-cropland model's performance in simulating crop growth and surface climate using multiple observational datasets, and (2) to investigate the extent to which dynamic

space crop growth alters irrigation effects on climate relative to a case with prescribed crop growth.

## 2 Methods

### 2.1 Regional climate model

For this study, we coupled the Community Land Model version 4 (CLM4) to WRF3.3 with a focus on improving crop process simulations within regional climate systems. CLM4 includes new treatments of soil column-groundwater interactions, soil evaporation, aerodynamic parameters for sparse/dense canopies, vertical burial of vegetation by snow, snow cover fraction and aging, black carbon and dust deposition, and vertical distribution of solar energy (Lawrence et al. 2012; Oleson et al. 2010). Simulations with CLM have been shown to improve daily temperature and precipitation when compared with

those with the Noah land surface model in an earlier version of WRF (WRF3.0-CLM3.5) (Jin et al. 2010; Lu and Kueppers 2012; Subin et al. 2011). However, we also found that CLM prescribed crop LAI in the Midwest was low compared to observations, potentially contributing to a large warm bias (Lu and Kueppers 2012). Further, in both Noah and CLM3.5, for natural vegetation and crops, plant parameters, such as leaf and stem area indices are fixed for each month of the year and do not have year-to-year variations. This limits applications of WRF3.0-CLM3.5 for studying two-way interactions between crops and climate.

To better simulate interactions between the atmosphere and cropland, we further developed a version of the coupled model (WRF3.3-CLM4crop) that simulates dynamic crop growth following work by Levis et al. (2012). The details of the crop growth parameterizations in the WRF3.3-CLM4crop are described in “Appendix” and are briefly summarized here. The crop growth module calculates the LAI, stem area index, canopy height, and carbon and nitrogen in

spaceleaf, stem, grain, and root at each time step based on environmental conditions. The LAI, stem area index, and canopy height are used in hydrology and radiation modules to calculate the energy and water state variables that are transferred into the atmospheric modules. LAI and plant carbon allocation differ according to phenological stage (planting, leaf emergence, grain filling, and harvest). Transitions between phenological stages are controlled by growing degree days (with a base of 8 °C for C3 crops and 10 °C for C4 crops). We used C3 and C4 crop types to represent the potential growth of major crops (e.g., C3 crops: wheat, soybean, and C4 crops: corn, sorghum). C3 and C4 crops differ in their photosynthesis pathways. C3 photosynthesis is more efficient than C4 under cool, moist, and normal light conditions, but C4 photosynthesis is more efficient than C3 under high light intensity and high temperatures. In CLM4crop, C3 (Collatz et al. 1991; Farquhar et al. 1980) and C4 (Collatz et al. 1992) photosynthesis are represented by different parameterizations for stomatal resistance and photosynthesis, and also have different phenological thresholds.

## 2.2 Irrigation scheme

We developed a precision agriculture-type irrigation scheme, where the amount and timing of irrigation simulates efficient irrigation practices. Irrigation water is applied as a function of root water stress ( $\beta_r$ ), leaf

temperature ( $T_{veg}$ ), and LAI. The root water stress is monitored by  $\beta_r$ , which varies from near zero (dry soil) to one (wet soil). Leaf temperature also is used, not only to more realistically simulate irrigation processes (Howell et al. 1984; Wanjura et al. 1992), but to maintain optimum plant growth as well, because high leaf temperature can inhibit plant photosynthesis (Wise et al. 2004). Irrigation starts after leaf emergence ( $LAI > 0.1 \text{ m}^2 \text{ m}^{-2}$ ), and occurs when either plant water is low ( $\beta_t < 0.99$ ) or leaf temperature is  $> 35 \text{ }^\circ\text{C}$ . In irrigated cropland areas (Fig. 1a), we applied irrigation water to the top of the crop plants to represent sprinkler

space

**space**Fig. 1 Modeled domain showing **a** percent of cropland equipped for irrigation (%) within each grid cell (Siebert et al. 2005), and **b** mean 2004–2006 irrigation water applied (million gallons per day) simulated in WRF3.3-CLM4crop. The four AmeriFlux observational sites are indicated in **a**, Ne3 has the same location as Ne1

**space(a)**  
space

**(b)**

irrigation, a widely used irrigation method in the US (50 % of land equipped for irrigation in 2005 reported in <http://water.usgs.gov/edu/wuir.html>). The irrigated cropland area was derived from the 0.05° global irrigation map (Siebert et al. 2005), as updated in 2006 ([http://www.geo.uni-frankfurt.de/ipg/ag/dl/forschung/Global\\_Irrigation\\_Map/index.html](http://www.geo.uni-frankfurt.de/ipg/ag/dl/forschung/Global_Irrigation_Map/index.html)). The irrigation scheme dynamically determines when and where to apply irrigation water at a consistent rate of  $0.0002 \text{ mm s}^{-1}$ . We tested several different irrigation rates within the range of current irrigation systems (4–20 gallons per min per acre) and selected the rate ( $0.0002 \text{ mm s}^{-1}$ ) that yielded reasonable cumulative annual irrigation water use compared to USGS surveys. The simulated annual irrigation water use (Fig. 1b) is within 14 % of US water usage estimated by USGS for 2005 (Kenny et al. 2005). The range in annual simulated irrigation water use from 2004 to 2006 was 113–149 billion gallons per day (143 for 2005); the USGS survey estimates 128 billion gallons per day in 2005 (<http://ga.water.usgs.gov/edu/wuir.html>).

## 2.3 Experimental design

We set up two 10-year (2002–2011) simulations using WRF3.3-CLM4crop to evaluate crop growth (LAI and growing season length). One is the control simulation without irrigation (hereafter referred to as CROP), and the other includes irrigation (hereafter referred to as CROPIRR) to quantify irrigation effects on climate with dynamic crop growth. In addition, we set up two additional 5-year (2002–2006) standard simulations with (hereafter referred to as STDIRR) and without irrigation (hereafter referred to as STD) using the prescribed LAI version of the coupled model (WRF3.3-CLM4) to quantify a baseline for irrigation effects on climate. We compared CROPIRR-CROP and STDIRR-STD differences to understand the extent to which irrigation effects are altered by dynamic crop growth. Based on several 1-year test simulations evaluating model performance, the physical modules used in all simulations include the MYNN boundary layer scheme (Nakanishi and Niino 2006), the CAM longwave/shortwave radiation scheme (Collins et al. 2004), the new

Grell cumulus scheme (Grell and Devenyi 2002), and the Thompson microphysics scheme (Thompson et al. 2004). The simulations focused on the contiguous United States (US) with 25 vertical layers and a 50 km horizontal resolution. We interpolated (using the inverse distance weighting method) 0.5° CLM surface input data (including plant functional types, plant function type percent, LAI, and stem area index) into the model domain. We regridded National Centers for Environmental Prediction/Department of Energy Reanalysis II global data to our domain as lateral boundary conditions (Kanamitsu et al. 2002). For analysis, we removed eight grid cells from the full perimeter of the domain

space as a buffer, which diminished the original domain from

109 129 to 93 113 grid cells. The first 2 years of the simulations were discarded as spin-up; for LAI validation we used 2004–2011 output and other validation focused on 2004–2006.

## 2.4 Validation data

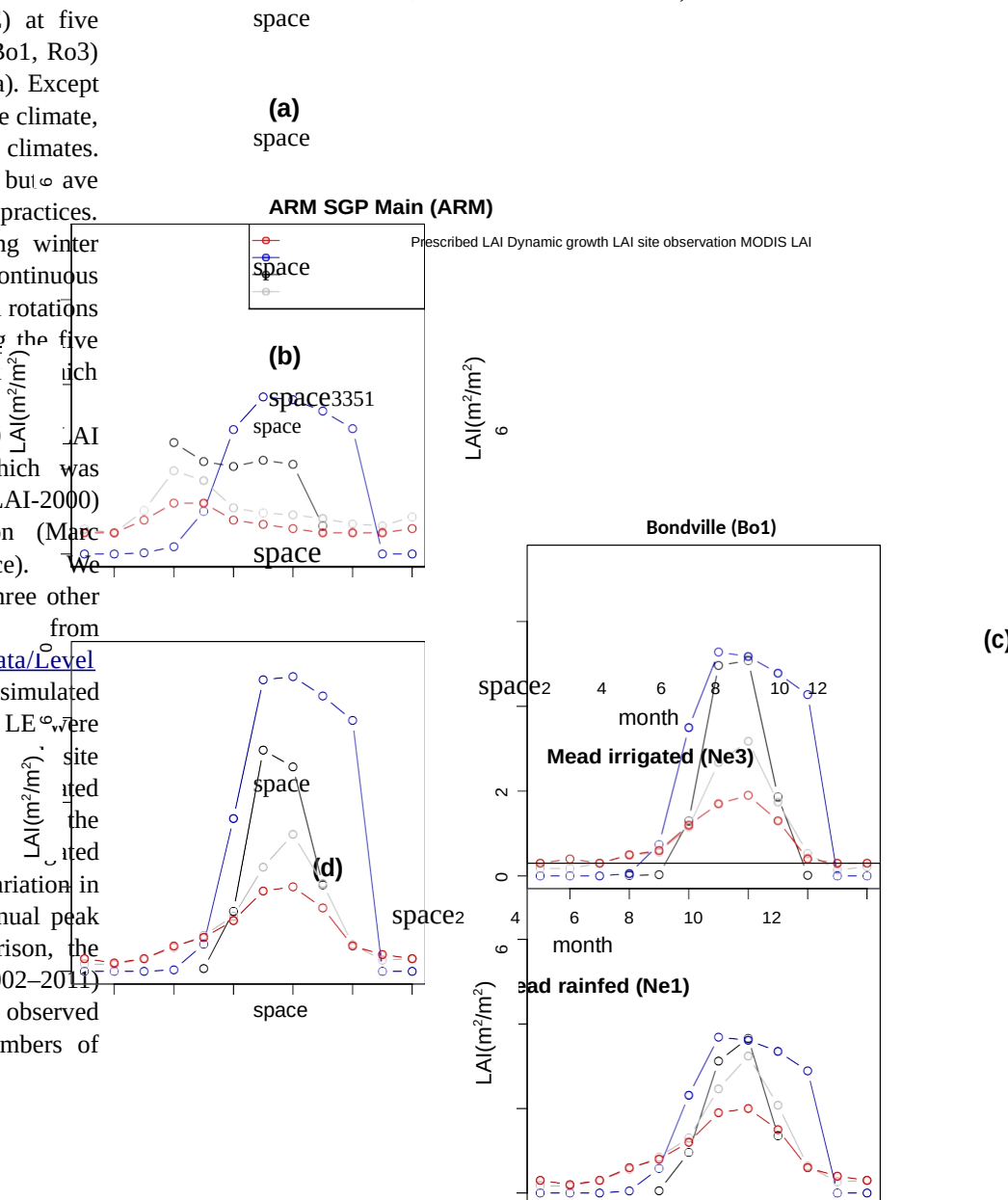
We validated the simulated LAI, sensible heat flux (H), and latent heat flux (LE) at five AmeriFlux sites (ARM, Ne1, Ne3, Bo1, Ro3) in the US Midwest (shown in Fig. 1a). Except for ARM, which has a semiarid steppe climate, all other sites have humid continental climates. These five sites all are agricultural but have different crop types and tillage practices. ARM has a periodic rotation among winter wheat, corn, and soybean; Ne1 has continuous corn; Bo1, Ro3, and Ne3 have annual rotations between corn and soybean. Among the five sites, only Ne3 is an irrigated crop site which is located 1.6 km away from Ne1.

We obtained 9-years (2002–2010) LAI data (Fischer 2005) at ARM, which was measured with a light wand (Licor LAI-2000) during the active growing season (March–Fischer, personal correspondence). We downloaded LAI measurements at three other sites (Bo1, Ne1, Ne3) from [ftp://cdiac.ornl.gov/pub/ameriflux/data/Level2/AllSites/biological\\_data/](ftp://cdiac.ornl.gov/pub/ameriflux/data/Level2/AllSites/biological_data/). The simulated LAI (for crop PFTs only), H, and LE were extracted at the grid cell nearest to site from the CROP simulations for non-irrigated sites (ARM, Bo1, Ne1, Ro3) and the CROPIRR simulation for the Mead irrigated site (Ne3). We compared monthly variation in LAI and interannual variation in annual peak LAI. For the monthly LAI comparison, the simulated LAI is the 10-year (2002–2011) averaged monthly LAI, while the observed LAI is averaged over different numbers of

years depending on availability of observations. We did not compare interannual variation in peak LAI at Bo1 because observations were only available for 5 years, 1997–2001. For H and LE, we compared the 3 year (2004–2006) averaged monthly model output to gap-filled level 2 AmeriFlux sites observations. Among the six levels of data provided by AmeriFlux, Level 2 is the standardized data that have been reviewed for consistent units, naming conventions, reporting intervals, and formats (<http://ameriflux.lbl.gov/data/aboutdata/>).

We used in situ soil moisture data from the international soil moisture network (<http://ismn.geo.tuwien.ac.at/>). Over the validation period of 2004–2006, the soil moisture measurements were available from Soil Climate Analysis Network (SCAN), Snow Telemetry (SNOTEL), Atmospheric Radiation Measurement (AtmRM), and AmeriFlux network. These networks measured the soil moisture at different depths, which cannot be directly compared to the ten soil depths in WRF3.3-CLM4crop. Therefore, we

**Fig. 2** Simulated monthly LAI compared to observations at four AmeriFlux sites. Modeled and MODIS LAI are averaged for 2002–2011, and observed LAI is averaged for 2002–2010 for ARM SGP main site, 2002–2007 for Mead irrigated and rainfed sites, and 1997–2001 for Bondville)



variation in peak LAI better than the simulation with prescribed LAI (Fig. 3), which has no inter-annual variation. Furthermore, dynamic crop with irrigation (CROPIRR) simulated the reduced interannual variability in peak LAI at the Mead irrigated relative to the Mead rainfed site. The standard deviation of peak LAI was  $1.09 \text{ m}^2 \text{ m}^{-2}$  smaller in the model and  $0.09 \text{ m}^2 \text{ m}^{-2}$  smaller in the observations in the Mead irrigated relative to the Mead rainfed site. The tenfold higher reduction in simulated standard deviation at the Mead irrigated site is

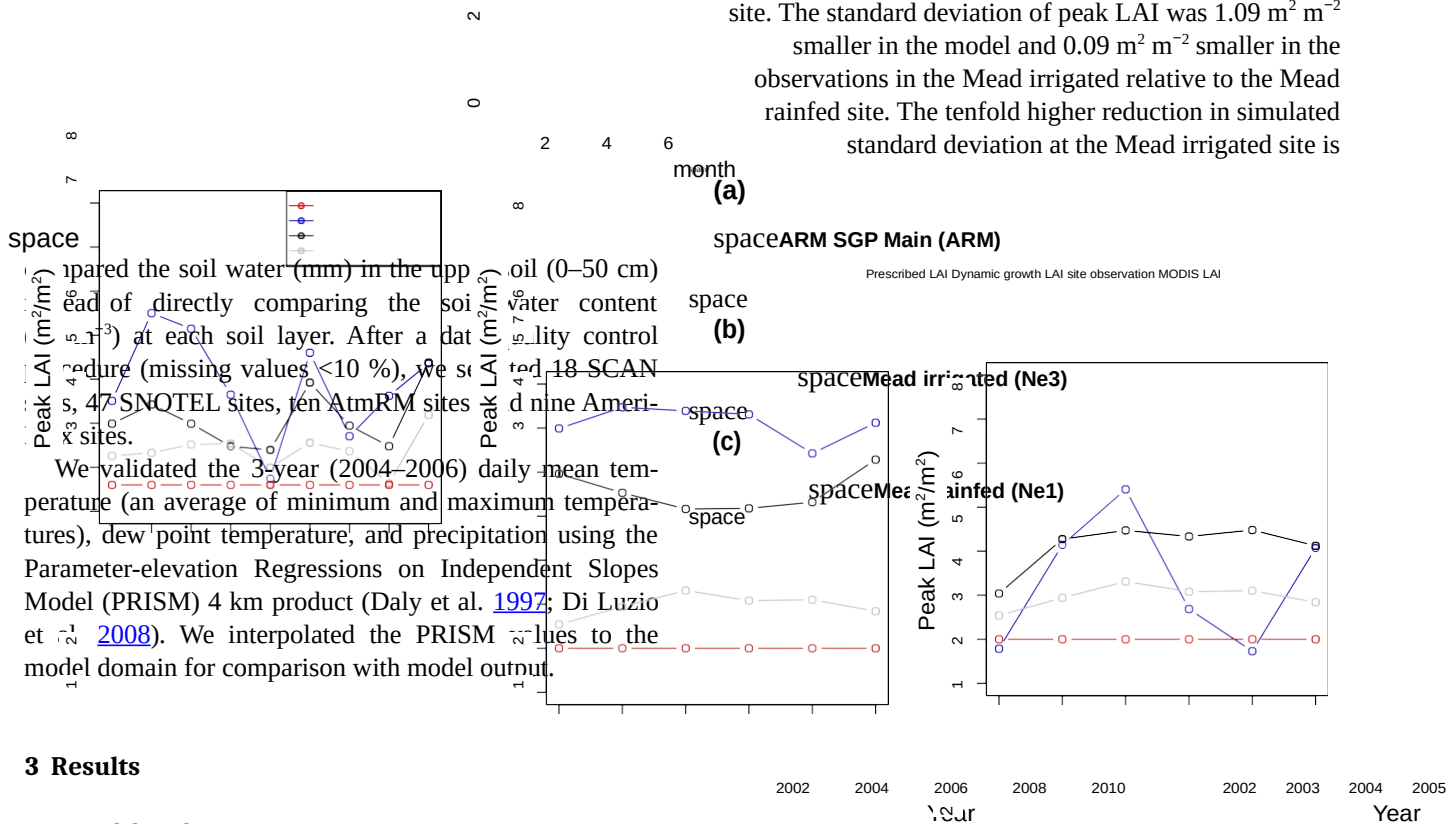


Fig. 3 Variation in simulated annual peak LAI compared to three AmeriFlux sites

### 3 Results

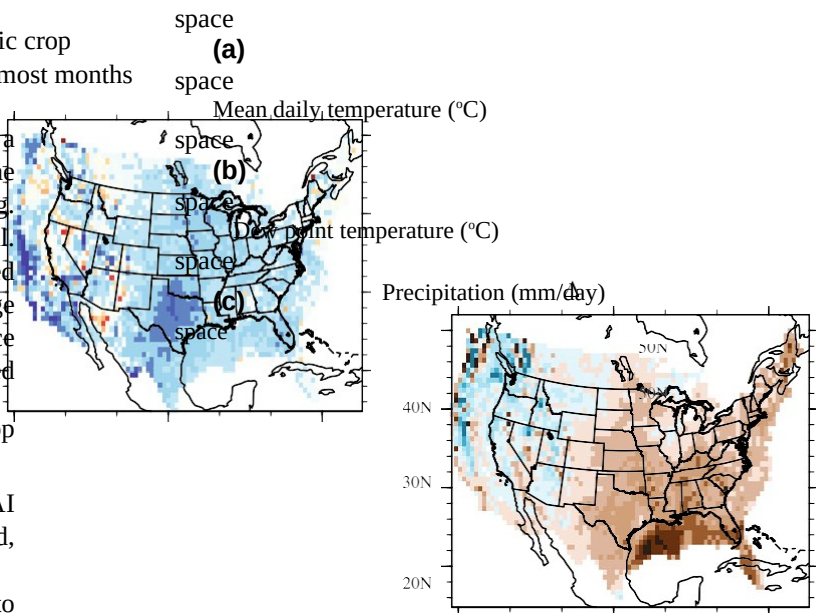
#### 3.1 Model evaluation

##### 3.1.1 Crop growth

Compared to the site observations, the dynamic crop growth model overestimated monthly LAI in most months and sites (58 % higher in average), displayed a longer growing season, but simulated the pattern of LAI increasing with irrigation (Fig. 2). The prescribed and MODIS LAI (Zhu et al. 2012) are smaller than the site-level observed LAI during summer by 52 and 38 % on average for the four sites, and showed no difference between the Mead irrigated (Ne3) and rainfed (Ne1) sites. Even though the dynamic crop

growth model overestimated the LAI magnitude at Mead irrigated and Mead rainfed,

it simulated a similar increase in LAI due to irrigation as in the site-level observations (29.8 % higher modeled vs. 29 % higher observed). Although the dynamic crop simulation (CROP) over-estimated peak LAI in some years, it captured the inter-annual



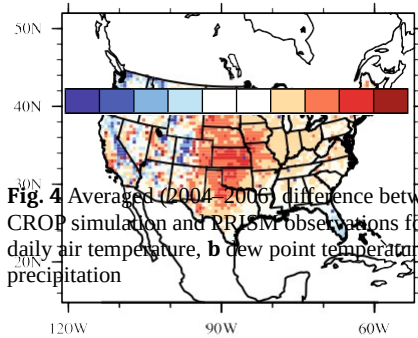


**Fig. 4** Averaged (2004–2006) difference between the CROP simulation and PRISM observations for **a** mean daily air temperature, **b** dew point temperature, and **c** precipitation

**Table 1** Spatially averaged root mean square error (RMSE) for maximum temperature (Tmax), minimum temperature (Tmin), mean temperature (Tmean), dew point temperature (Td), and precipitation (ppt)

space between PRISM and the four simulations (STD, STDIRR, CROP, and CROPIRR) in 2004–2006

	All domain				Non-irrigated cropland Irrigated cropland		
	STD	STDIRR	CROP	CROPIRR	STD	STDIRR	CROPIRR
Tmax (°C)	3.51	3.29	3.47	3.42	3.57	3.24	3.49
Tmin (°C)	2.82	2.68	2.53	2.47	2.43	2.27	2.01
Tmean (°C)	2.71	2.51	2.48	2.41	2.62	2.35	2.29
Td (°C)	2.7	2.76	2.71	2.69	2.35	2.42	2.28
ppt (mm/day)	1.25	1.22	1.22	1.22	1.32	1.27	1.28

space due to overestimated interannual variation in peak LAI at the Mead irrigated site, which is likely due to an overestimate of interannual variation in precipitation by 26.6 %. This greater variation in precipitation resulted in a large variation in plant-available water and therefore higher peak LAI in some years (Fig. 3c).

The dynamic crop growth model simulated an earlier planting date for most C3 crops and some C4 crops than observed soybean and maize planting dates available from USDA crop calendar surveys summarized in Sacks et al. (2010). Simulated planting dates were within the observed planting date range for 34 % of C3 and 62 % of C4 cropland. For the C3 cropland, the model simulated too-early planting by 5–6 days in the remaining 66 % of C3 crop area. For the C4 cropland, the model simulated too-early planting by 6–10 days in 38 % of the C4 crop area, mostly in the Midwest and East. Only 1.1 % of the simulated C4 cropland had later than observed planting dates, by 7–13 days in Montana and Wyoming.

### 3.1.2 space Surface climate and energy fluxes

The CROPIRR simulation overestimated the annual average mean daily temperature (Tmean; Fig. 4a) in the Midwest by up to 3.5 °C. The largest monthly warm bias (7 °C) was in July and the smallest (0.5 °C) was in March. These warm biases were larger—by an additional

1.4 °C in JJA average—without irrigation in CROP (the July bias increased by up to 3.3 °C). The warm bias in CROPIRR was reduced by 2–5 °C from the previous version of the coupled model (Lu and Kueppers 2012). Dew point temperature (Td) was underestimated in most regions (Fig. 4b), indicating low humidity in the model simulations even with irrigation. For 18 % of the continental US, this underestimation was strongly correlated ( $r > 0.8$ ) to the low precipitation bias. Precipitation (ppt; Fig. 4c) was underestimated in the Midwest and Eastern US and overestimated in the Western US by up to 2 mm day<sup>-1</sup>. Where the model simulated excessive precipitation in the

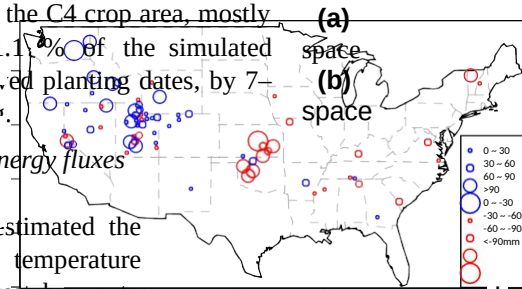
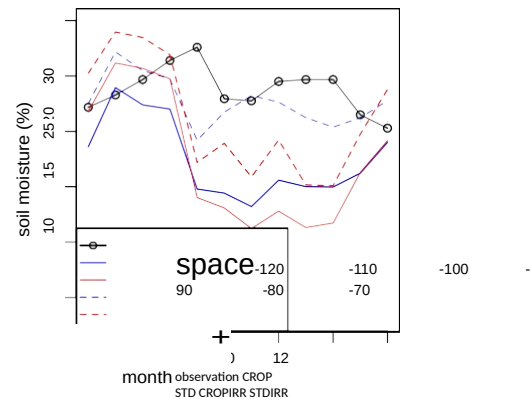


**Fig. 5** Comparison of simulated and observed soil moisture. **a** Soil water (0–0.5 m) difference between CROP and observed and **b** soil moisture comparison at the Mead irrigated site



space Western US, there was a cold bias, and the low Td was due to underestimated air temperature since Td never exceeds air temperature.

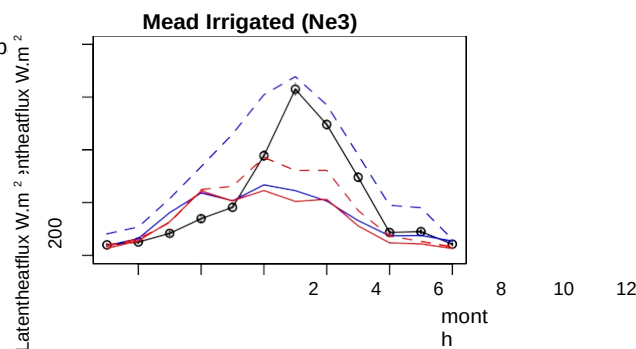
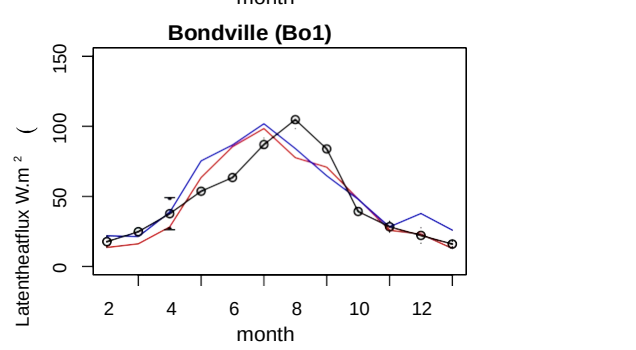
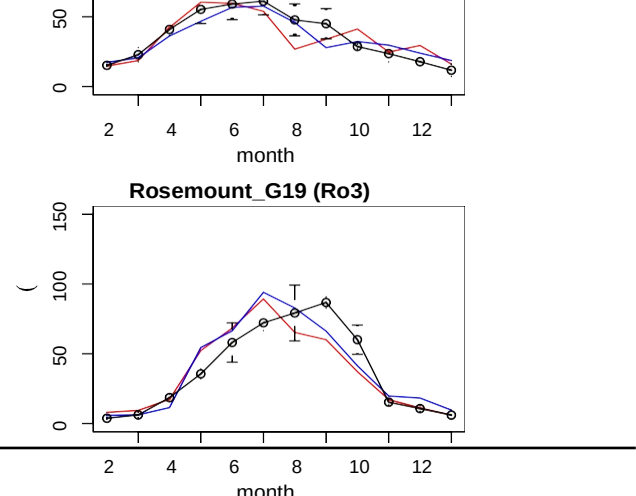
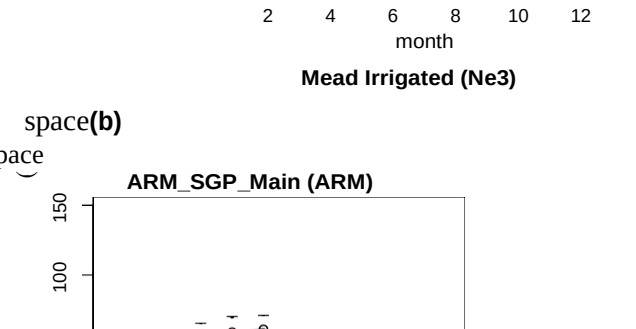
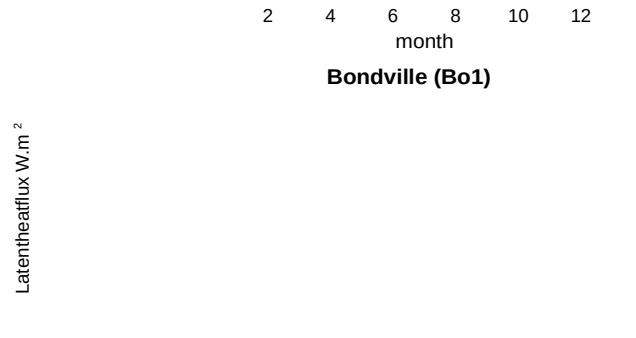
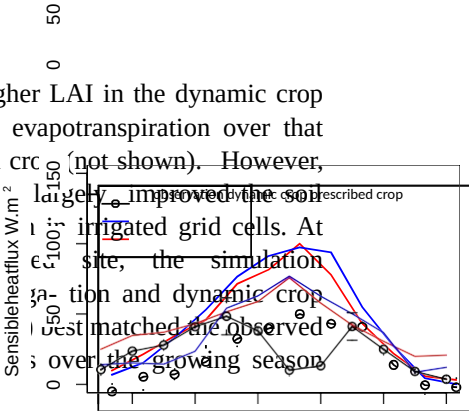
Adding a crop growth model and irrigation improved domain average Tmin the most relative to other variables listed in Table 1 (RMSE was reduced by 18 % for Tmin, 16 % for Tmean, 6 % for Td, 4 % for Tmax, 2 % for ppt from STD to CROPIRR). However, the Tmin RMSE was still higher in irrigated than non-irrigated grid cells (Table 1). In general, the improvements tend to be greater over irrigated land. The RMSE of Tmax is always greater than the RMSE of Tmin no matter which simulation or subset grid cells, and it only is slightly improved by adding crop growth and irrigation for non-irrigated (1.7 %) and irrigated land (3.7 %). Similar to Tmax, Td and precipitation are not substantially improved in CROPIRR.

The coupled model generally over-predicted 0–50 cm soil water by 20 mm in the Western US and under-predicted soil water in the Midwest by 49 mm and Eastern US by 20 mm when compared to site level observations (Fig. 5a). CROPIRR showed the best simulation of soil water among all four simulations. Adding the dynamic crop model did not improve the soil moisture simulation everywhere; at some sites, the low soil moisture bias was exacerbated

space because higher LAI in the dynamic crop model increased evapotranspiration over that in the prescribed crop (not shown). However, adding irrigation largely improved the soil moisture simulation in irrigated grid cells. At the Mead irrigation site, the simulation including both irrigation and dynamic crop growth (CROPIRR) best matched the observed soil moisture level over the growing season (Fig. 5b).

Incorporating only dynamic crop growth into the model does not substantially improve simulated surface energy fluxes, but the addition of irrigation does. Both STD and CROP simulated higher sensible heat flux (H) than observed at all four Ameriflux sites (Fig. 6) and do not capture the double peak pattern at Bondville (Bo1) and Mead Irrigated (Ne3). There was only slight improvement in simulated H at Rosemount G19 (Ro3) and Ne1 sites. CROP simulated higher latent heat flux (LE) than STD, but still produced a peak in LE that was 1 month earlier than observed at Bo1 and 2 months earlier at Ro3. With the addition of irrigation, biases in H and LE at the Mead irrigated site were reduced most in CROPIRR. The double peak pattern of H and the peak month of LE were well simulated by CROPIRR, but were not captured in STDIRR, which lacks a dynamic crop growth model.

space3354  
Y. Lu et al.



space

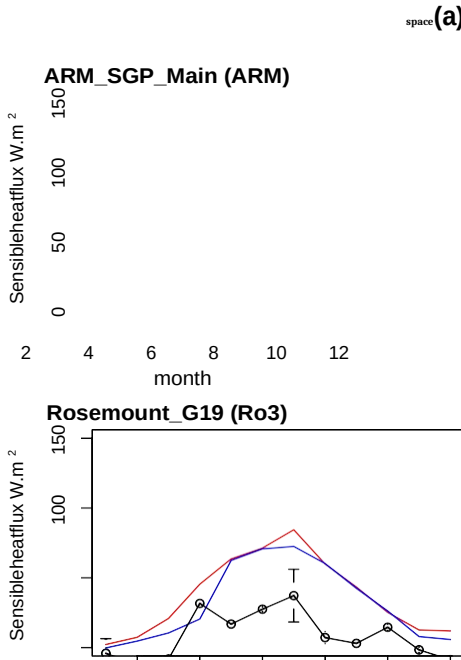




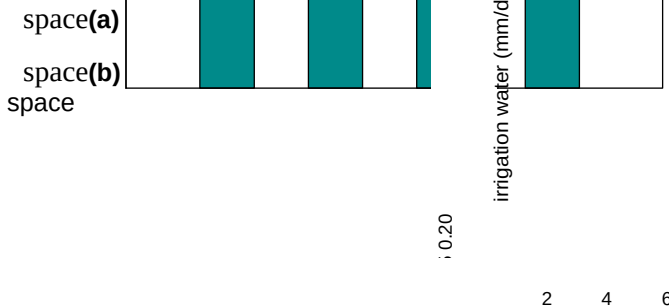
**Fig. 6** Comparisons of 2004–2006 monthly mean sensible heat flux (a) and latent heat flux (b) between model simulations and observations at four AmeriFlux sites

### 3.2 The role of dynamic crop growth in climate effects of irrigation

We compared the differences between the simulated surface variables for the period of 2004–2006 to quantify how dynamic crop growth influences irrigation effects on surface energy fluxes and temperature. Dynamic crop growth

requires more irrigation water during the growing season than prescribed crop growth (Fig. 7a). From April to September, the irrigation water applied in the CROPIRR simulation is almost twice than in STDIRR. In winter, the simulation with prescribed crop had high irrigation water use ( $0.05 \text{ mm day}^{-1}$ ) because the dynamic crop module in CROPIRR does not simulate winter crops or cover crops and

**Fig. 7** Monthly variation in domain averaged a irrigation water (mm/day) and b leaf area index ( $\text{m}^2/\text{m}^2$ ) in prescribed crop and dynamic crop simulations



space

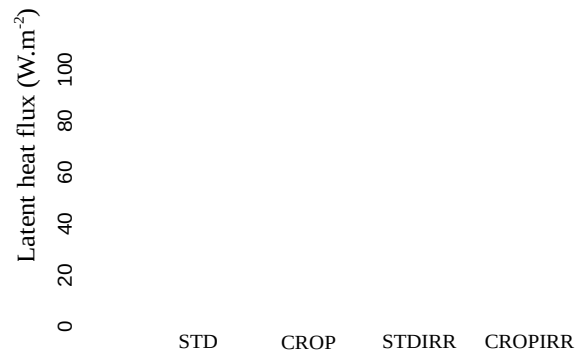


**Fig. 8** Simulated 2004–2006 averaged latent heat flux partitioned into three components for the four models

does not apply irrigation water from November to February. When comparing the two simulations with dynamic crop growth (CROPIRR vs. CROP), LAI was 29.8 % greater with irrigation, while LAI did not change with irrigation under prescribed LAI (STDIRR vs. STD) (Fig. 7b). This increase in LAI due to irrigation is comparable to observations (29 % greater LAI at Mead irrigated than Mead rainfed, Fig. 2c, d).

Dynamic crop growth plus irrigation improved the simulated partitioning of surface energy fluxes. In CLM, the latent heat flux was partitioned into soil evaporation, wet leaf evaporation, and dry leaf transpiration. Because the LAI does not change with the prescribed crop, a large fraction of the water applied to the soil column evaporated from the soil. In STDIRR, 50 % of the total evapotranspiration was soil evaporation and 35 % was leaf transpiration (Fig. 8). In the simulation with dynamic crop growth, the increase in LE with irrigation is mainly due to increased leaf transpiration resulting from the larger leaf area; soil evaporation is only a small portion of LE.

The averaged JJA differences (irrigation run–non irrigation run) in climate variables with irrigation have a similar pattern

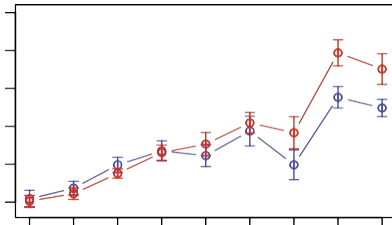
spacebut a different magnitude in the prescribed and dynamic crop growth cases as the cell-fraction of irrigated cropland increased (Fig. 9). Irrigation increased LE and reduced H, but these effects are 34.6 % greater for  $\Delta H$  and 24.6 % greater for  $\Delta LE$  with dynamic crop in moderately irrigated regions (20–50 % irrigated). Irrigation increased net radiation similarly in STDIRR and CROPIRR, except when irrigation area was >60 %, when the increase in net radiation is 41.9 % smaller with dynamic compared to prescribed crops. Irrigation reduced 2-m air temperature (due to less sensible heat flux) more strongly in CROPIRR than in STDIRR when grid cell percentage irrigated was >15 %.

## 4 Discussion and conclusions

### 4.1 Model evaluation

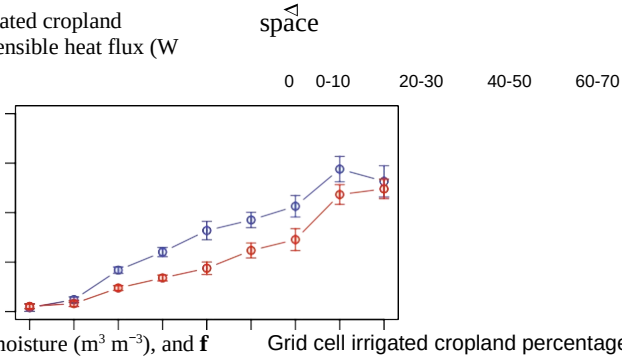
By coupling CLM4Crop into WRF (version 3.3), we have taken the first step toward extending the capability of WRF to simulate the two-way interactions between crop growth and climate. As one of the most widely used regional climate models, it is important that WRF have a comprehensive land surface model option. Jin et al. (2010) first coupled the CLM (version 3) into WRF (version 2) and then Subin et al. (2011) updated the coupled model (WRF3.0–CLM3.5). We further updated the coupled model to WRF3.3–CLM4 and incorporated a dynamic crop growth scheme to better reflect seasonal changes in LAI, and added an irrigation scheme to capture large effects of increased soil moisture on surface energy and water fluxes.

Our surface energy flux evaluation suggested that improvements to dynamic crop growth are not sufficient to better simulate energy fluxes; improvements to other physical processes (such as precipitation) are equally important. We expected the larger and more dynamic



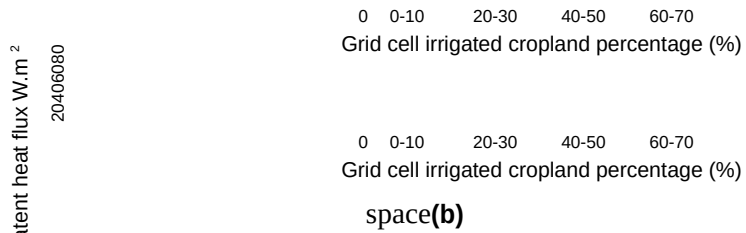
LAI simulated in CROP to improve simulation of surface energy fluxes where the prescribed LAI was small

**Fig. 9** 2004–2006 JJA averaged difference along different grid cell irrigated cropland percentage of **a** latent heat flux ( $W m^{-2}$ ), **b** sensible heat flux ( $W m^{-2}$ ), **c** net radiation



( $W m^{-2}$ ), **d** 2 m air temperature ( $^{\circ}C$ ), **e** soil moisture ( $m^3 m^{-3}$ ), and **f** Bowen ratio reduction (%) in prescribed crop and dynamic crop simulations. The error bar shows the standard error among 9 months

space(a)



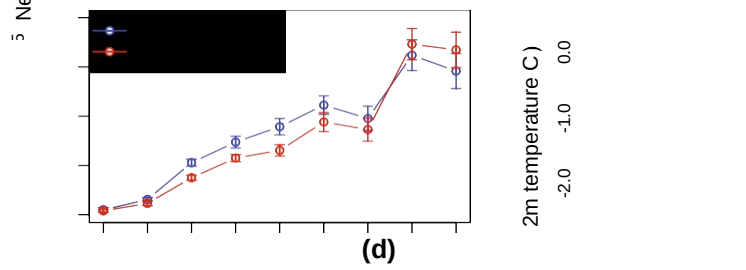
(c)

( - )



Δ

(e)



20 Soil moisture ( $m^3 m^{-3}$ )

(f)  
space

0 0-10 20-30 40-50 60-70  
Grid cell irrigated cropland percentage (%)

0 0-10 20-30 40-50 60-70  
Grid cell irrigated cropland percentage (%)

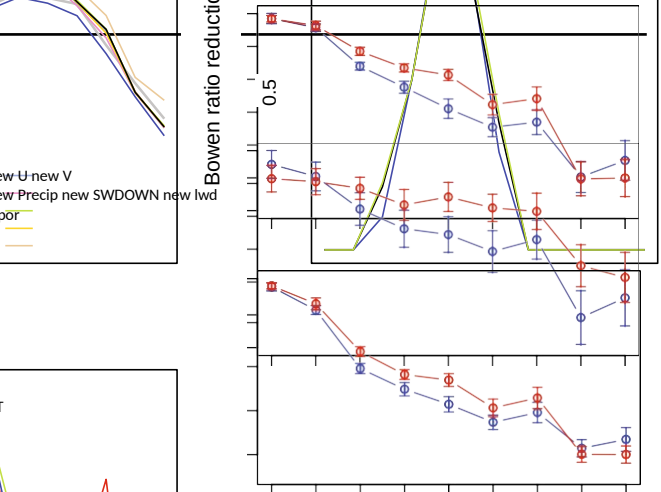
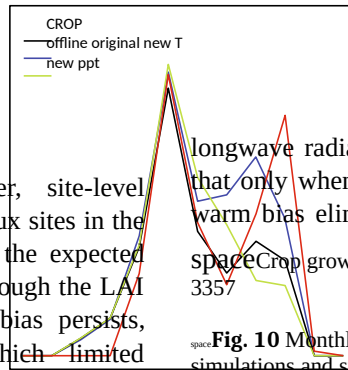
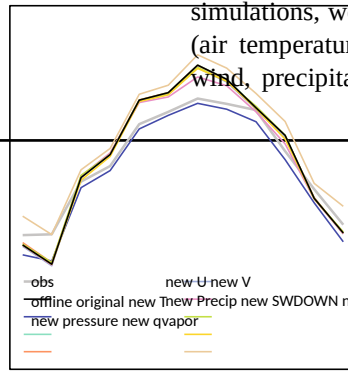
0 0-10 20-30 40-50 60-70  
Grid cell irrigated cropland percentage (%)

space

space compared to observations. However, site-level comparisons to three non-irrigated AmeriFlux sites in the Midwest suggest that we did not realize the expected improvements. The reason may be that although the LAI is larger in CROP, the low precipitation bias persists, resulting in the low soil moisture, which limited evapotranspiration regardless of the LAI. This is accompanied by an underestimated cloud cover and overestimated downward solar radiation (not shown), biases persisting in the previously coupled version (Lu and Kuepper 2012). As a consequence, gross energy fluxes (latent heat flux, sensible heat flux) and the Bowen ratio RMSEs in CROP comparable to those in STD at ARM and Bo1. However, when irrigation was applied at the Ne1 site, surface energy flux partitioning was substantially improved. Therefore, we suspect that in regions with a dry bias, if the precipitation simulation could be improved, the simulated surface energy fluxes and flux partitioning will also be improved.

Even though the warm bias in air temperature was reduced relative to the previous version of the coupled model, there is still unresolved warm bias in the Midwest. In the previous version (WRF3.0-CM3.5), there was a very large warm bias of 4 to 10 °C in the Midwest (Lu and Kuepper 2012). This warm bias was reduced by 2-3 °C by updating the land surface model, as well as by using the MYNN boundary layer scheme in STD. It was further reduced by 1-2 °C when adding dynamic crop growth model and irrigation processes. To diagnose the source of the warm bias, we conducted nine 1-year (2004) offline CLM simulations at the ARM

site. The original offline test was driven by the 6 h output from the CROP simulation. Then in the remaining eight simulations, we replaced one of the eight forcing variables (air temperature, surface pressure, water mixing ratio, wind, wind, precipitation, downward solar radiation, downward

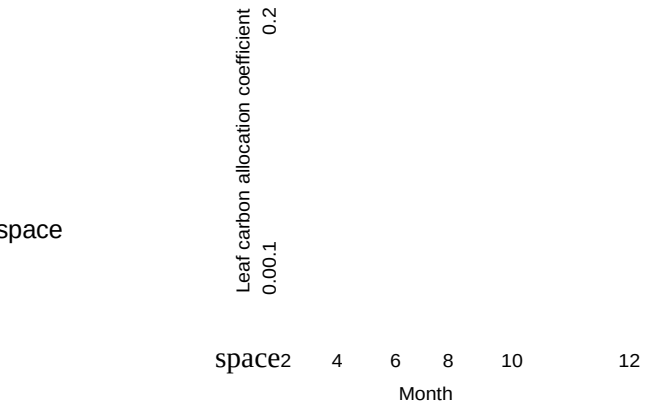


longwave radiation) with the site observations. We found that only when using observed air temperatures was the warm bias eliminated,

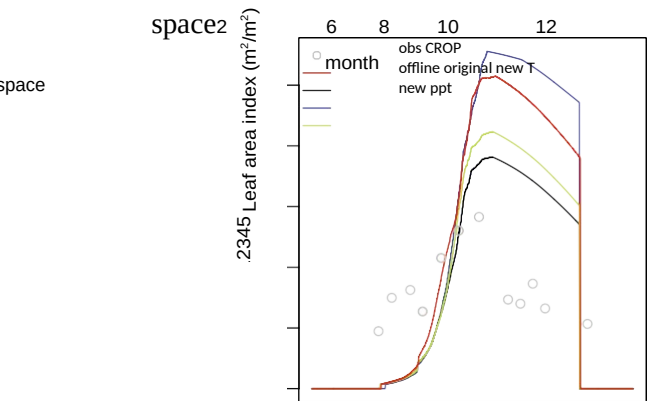
Crop growth and irrigation

Fig. 10 Monthly variation of 2-m air temperature for the eight 1-year offline simulations and site observation

(a)  
(b)  
space



(d)



space even though the forcing data still have biases in other driving variables, such as large downward radiation and low precipitation (Fig. 10a). Replacing these other driving variables did not reduce the warm bias, but did improve surface energy fluxes. For example, replacing model precipitation with site precipitation in the forcing data increased the LE and reduced H, and using the site downward solar radiation largely reduced H (not shown). These offline simulations indicated that the unresolved warm bias in the coupled model came from the warm bias in the lowest level atmosphere temperature (24–30 m above the land with spatial variations) that cannot be removed by improvements to the land surface model.

The summer dry bias in the central US is mainly due to poor simulation of the Great Plain Low Level Jet (GPLLJ), which is defined by the 925 mb meridional wind averaged across 25°N–35°N and 100°W–95°W (Zhang et al. 2009). The GPLLJ plays an important role in summertime precipitation and moisture transport over the Central US (Higgins et al. 1997). In NARR and NCEP2 reanalyses, the summer GPLLJ ranges from 4 to 7 m s<sup>-1</sup> and the Central US precipitation ranges from 3 to 5 mm day<sup>-1</sup>. The GPLLJ in our best simulation (CROPIRR) is only around 2 m s<sup>-1</sup>,

and the summer precipitation is about 1–2 mm day<sup>-1</sup>. From spring to summer, the GPLLJ in NARR and NCEP2 gradually increased and reached a peak in June, while in our model, the GPLLJ increased from January to March and then decreased. The underlying mechanism of why the model cannot realistically simulate the strength of the meridional wind from April to August is beyond the scope of this paper. For the Southeast US, the dry bias is due to the incorrect simulation of the western ridge of the North Atlantic subtropical high. Li et al. (2014) found a similar dry bias in summer precipitation to be because the western ridge of the North Atlantic subtropical high in WRF simulations shifts 7° northwestward compared to the reanalysis ensemble. In our simulations, we found a similar northwestward shift of the western ridge.

The warm and dry bias in WRF-CLM affected crop growth by advancing the grain fill phenology phase, increasing leaf carbon

allocation coefficients, and reducing net primary production (NPP). As described in the above offline tests, keeping other forcing variables the same, we found that crop growth in the offline simulation driven by the modeled temperature (with warm bias) has an earlier grain fill by 33 days for C3 crop and by about 25 days for

C4 crop as compared to the offline simulation driven by the observed temperature (without warm bias). The warm bias also increased the leaf carbon allocation coefficient by 5.7 % for C3 crop and 3.8 % for C4 crop (Fig. 10b). The warm and dry conditions limit the maximum rate of carboxylation ( $V_{cmax}$ ) and therefore reduced plant photosynthesis. NPP was reduced by 33 and 4 % for C3 and 16 and 13 % for C4 (Fig. 10c) with warm bias and dry bias respectively. A similar offline test at Ne1 sites showed similar decline of NPP due to warm bias (69 % lower for C3 and 59 % lower for C4 at Ne1). This result indicates that C3 and C4 crop growth are both sensitive to atmospheric model biases. We expect improvements in crop growth simulation with reduced warm and dry bias, especially for the C3 crop because C3 photosynthesis is more limited in dry and warm conditions.

The overestimated LAI in WRF3.3-CLM4crop is not due to the warm and dry biases, which would reduce NPP as described above. We found that the offline simulations have a smaller LAI than the coupled simulation (CROP). The mean LAI bias at ARM in 2004 is 0.06 m<sup>2</sup>/m<sup>2</sup> for the offline simulations but increased to 0.7 m<sup>2</sup>/m<sup>2</sup> for the coupled simulations (Fig. 10d). Differences in atmospheric forcing between the offline and coupled models may have contributed. For example, photosynthetically active radiation was calculated as a constant rate of the total downward solar radiation in the offline simulations, but the coupled model used a dynamic calculation in the radiation scheme. Nevertheless, the overestimate of LAI in both offline and coupled models indicates that the crop models still need improvements, which in turn requires high temporal resolution observations such as crop phenology, crop NPP, across leaf carbon at a broader range of sites.

Comparing to CESM1 (Levis et al. 2012), WRF3.3-CLM4crop has similar biases in crop growth even with the modified carbon allocation parameters. Both models overestimated the LAI and growing season length. CESM1 simulated a higher LAI for soybean (C3 crop) than for maize (C4 crop) and our model displayed similar results. Mean C3 LAI was greater than C4 LAI by 0.19 but with clear spatial variation (higher C3 LAI in the northern US and higher C4 LAI in the southern US). Excluding the soil carbon and nitrogen calculations from WRF3.3-CLM4crop limits its capability for studying biogeochemical interactions between cropland and climate. Levis et al. (2012) found that adding dynamic crop growth resulted in stronger improvements in the simulations of biogeochemical variables (such as NEE) versus biogeophysical variables (such as H and LE). Our current version of the model can be only used to study biogeophysical interactions between climate and cropland. Furthermore, the root distribution parameters (Zeng 2001) were not updated as crops developed throughout the growing season in either model. In future versions, a root growth submodel is needed to better capture the relationship between crop growth and root water uptake.

Irrigation increased latent heat flux (LE), comparably to that generated by other similar models with precision irrigation schemes run over the US. Irrigation produced an increase in JJA LE of  $21.4 \text{ W m}^{-2}$  under prescribed crop and  $30.8 \text{ W m}^{-2}$  with dynamic crops over irrigated land. Harding and Snyder (2012b) simulated an increase in JJA LE of  $21 \text{ W m}^{-2}$  using the standard WRF, Sacks et al. (2009) simulated an increase in JJA LE  $20\text{--}30 \text{ W m}^{-2}$  using CCSM, and Cook et al. (2011) simulated an annual increase in LE by  $16\text{--}20 \text{ W m}^{-2}$  using GISS ModelE. Previous work using simpler irrigation schemes applied in arid and semi-arid regions produced much greater increases in LE. For example, Kueppers et al. (2007) simulated a  $152 \text{ W m}^{-2}$  (20 years JJA average) increase in LE in California, and De Ridder and Gallee (1998) simulated a  $75 \text{ W m}^{-2}$  (at midday) increase in LE in southern Israel. In observations, LE is  $16.5 \text{ W m}^{-2}$  higher on average in JJA at Mead irrigated sites compared to that at Mead rainfed sites; we would expect there to be site-to-site variation in this value.

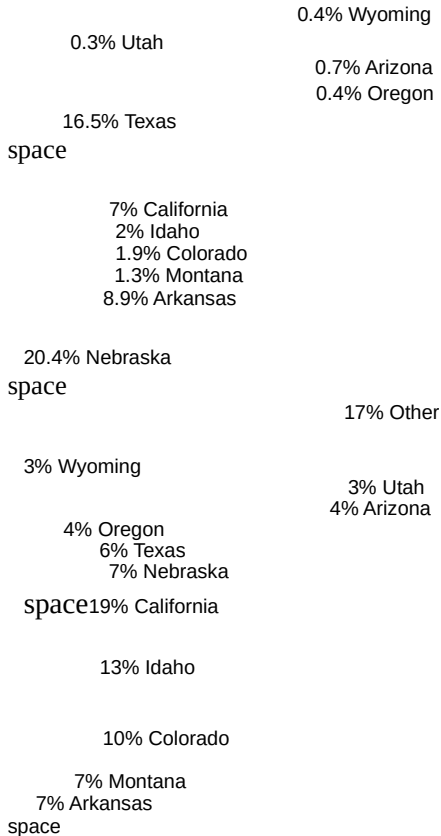
#### 4.2 The role of dynamic crop growth in climatic effects of irrigation

Our results suggest that the dynamic crop growth model is important for evaluation of irrigation effects on climate. Without dynamic crop growth, models could underestimate the irrigation effects on climate in moderately (20–50 % irrigated cropland) irrigated regions (Fig. 9). This is due to the amount of irrigation water applied. On average, simulations with dynamic crop growth required more irrigation water (Fig. 7a) and therefore resulted in greater increases in soil moisture and LE, and greater decreases in H, T2, and Bowen ratio in moderately irrigated cropland. In addition, the dynamic crop growth simulation had a more reasonable simulation of latent heat flux components, with higher latent heat flux resulting from increased leaf evapotranspiration, not increased soil evaporation as occurred with prescribed LAI. Such increased soil evaporation is not reasonable because observations have shown that soil evaporation is about 30 % of evapotranspiration for irrigated cropland (Lascano et al. 1987).

Our simulation used a precision irrigation practice and the amount of annual irrigation water over the entire domain was validated

with a USGS irrigation survey. However, the amount of water added to each state differed substantially from the USGS irrigation survey (Fig. 11). This is due to model biases in soil moisture. For example, too much irrigation water was added to Texas and Nebraska

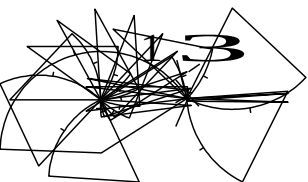
**Fig. 11** State level irrigation percentages for model space (CROPIRR) and USGS in 2005. The total amount applied is 143 million gallons per day in CROPIRR, and 128 million gallons per day according to the USGS survey



in the model because the dry bias in this region resulted in insufficient soil water to support crop growth, while less irrigation water was applied in western states, such as California, Idaho, and Colorado due to the wet biases in these states. Therefore, ensemble simulations with multiple regional climate models and irrigation schemes may be required to average over model biases and accurately quantify the effects of irrigation on surface climate.

#### 4.3 Conclusions

In summary, this work evaluated the performance of a coupled crop-climate model (WRF3.3-CLM4crop) in the simulations of crop growth and surface climate. We found that the coupled model overestimated crop LAI and growing season length but displayed a reasonable interannual variability. Adding both the dynamic crop model and the irrigation scheme improved model simulation of temperature and precipitation within and beyond agricultural regions. Adding irrigation reduced the dry bias in irrigated cropland and



greatly improved the energy flux simulation at the Mead irrigated site, while the improvement was limited in other regions by the model's dry bias. A dynamic crop growth model is important for evaluation of crop management effects on climate. Excluding dynamic crop growth underestimated irrigation water demands and climate effects of irrigation in moderately irrigated regions.

**Acknowledgments** We thank for Samuel Levis for providing the CLM4CNCrop code, Marc Fisher for providing the ARM SGP Main site LAI observations, UC Merced for summer GRC fellowships, and an anonymous reviewer for helpful comments. The work was also supported by USDA AFRI (Award Number 2012-68002-19872).

## Appendix: Dynamic crop module in WRF3.3-CLM4crop

We incorporated the dynamic crop growth module from CLM4CNCrop into the coupled regional model WRF3.3-CLM4. The dynamic crop growth module is based on AgroIBIS (Kucharik 2003) and described in detail in Levis et al. (2012).

### spaceModifications

We made several modifications to the dynamic crop module to better fit into the coupled regional model framework. First, we fixed the soil carbon and nitrogen state variables. In the original CLM4CNCrop model, crop growth is linked to the carbon and nitrogen model, which updates multiple soil and plant carbon and nitrogen variables at each time step based on crop phenology and environmental changes. It requires a long spin-up time (over 1000s of years) to enable the soil carbon and nitrogen to reach current steady states. For a high-resolution regional climate model, such long spin-up simulations are difficult with current computing resources. Further, even though soil carbon and nitrogen are simulated in CLM4CNCrop, these values would not be routinely coupled to atmospheric carbon and nitrogen in a regional model. Because our regional scale focus is on biogeophysical, not biogeochemical feedbacks, between land and atmosphere, we assumed that for crops, the soil carbon and nitrogen could be maintained at optimum levels year-year.

Second, at this stage, we consider WRF3.3-CLM4crop able to simulate C3 and C4 crops, not specific crop types. The current version of CLM4CNCrop simulates three crops (summer cereal, soybean, corn). The growth of these

crops is strongly dependent on photosynthetic pathway. We assume that at a regional scale, it is inappropriate to expect the model to simulate specific crops across the domain with validation only at one or several grid cells where observations are available. Therefore, we used C3 and C4 crop types to represent the potential growth of major crops (e.g., C3 crops: wheat, soybean, and C4 crops: corn, sorghum). The next phase of our work will aim to gather more observations and validate growth parameters for more specific crop types.

Third, we made changes to crop phenology and carbon allocation to better suit the regional coupled model framework and applications. In the planting phase, we changed the 20-year running mean growing degree days into 5-year running mean growing degree days to better match our simulation period. In the harvest phase, we assumed harvest

### space3360

Y. Lu et al.

space occurs when the crop reaches 1.5 times the GDD required for maturity rather than occurring as soon as the crop reaches maturity as in CLM4CNCrop, since some crops such as corn (Nielsen 2011) are left in the field after maturity to dry. We also modified the carbon allocation to better reflect environmental stress on crop growth as described in section A3 of the appendix.

### Phenology

#### Planting

The thresholds for planting, and thus initiation of the crop development cycle, are defined as:

$$T_{2m} > T_p$$

$$GDD_8 > GDD_{min}$$

where  $T_{2m}$  is the instantaneous 2-m air temperature (°C),  $T_p$  is a crop-specific planting temperature (7 °C for C3 crop and 10 °C for C4 crop),  $GDD_8$  is the 5-year running averaged growing degree days (base 8 °C) from March to September, and  $GDD_{min}$  is the minimum growing degree day requirement (50 degree days for both C3 and C4 crops). C3 crop must meet the planting temperature requirement between March 1st and May 14th, and C4 crop between May 1st and June 14th.

At planting, some initial values are assigned, including leaf area index (0.1 m<sup>2</sup>/m<sup>2</sup>), stem area index (0.01 m<sup>2</sup>/m<sup>2</sup>), leaf carbon (3 gC/m<sup>2</sup>), stem carbon (3 gC/m<sup>2</sup>), and fine root carbon (4.5 gC/m<sup>2</sup>). The growing degree days value necessary for the crop to reach vegetative and physiological maturity,  $GDD_{mat}$ , is updated:

$$GDD^{c3crop} = 0.85GDD_8$$

$$GDD^{c4crop} = 0.85GDD_8$$

### spaceGrain fill

Grain begins to fill when the growing degree days since planting ( $GDD_{plant}$ ) reaches 70 % for C3 and 65 % for C4 crop of  $GDD_{mat}$ . The leaf area index and stem area index

decline and transfer some amount (defined in A3) of leaf and live stem carbon to grain.

### Harvest

We assumed harvest occurs when the crop reaches 1.5 times the GDD required for maturity ( $GDD_{plant} > 1.5GDD_{mat}$ ) rather than as soon as the crop reaches maturity as defined in CLM4CNCrop, because crops, such as corn were left in the field after maturity to dry (Nielsen 2011).

### CN allocation

Initial leaf carbon and nitrogen is assigned at planting. We adjusted the value from  $1\text{gC/m}^2$  in CLM4CNCrop to  $3\text{gC/m}^2$  because the small initial leaf carbon generated a too small leaf carbon, resulting in low LAI compared to observations and too little gross primary production (GPP) for carbon allocation. The initial leaf nitrogen was calculated using leaf C:N ratio from Levis et al. (2012). C and N allocation starts with leaf emergence and ends with harvest. Carbon allocation is based on allocation coefficients and the nitrogen is assigned based on the tissue (leaf, stem, root, and grain) C:N ratio.

### Leaf emergence to grain fill

The allocation coefficients to each C pool are defined as:

$$a_{grain} = 0$$

$$a_{froot} = 0.7(1 - \beta_p)$$

$$a_{leaf} = 0.5(1 - a_{froot})$$

$$a_{livestem} = 0.5(1 - a_{froot})$$

where  $GDD_8$  and  $GDD_{10}$  are the 5-year running averaged growing degree days from March to September.

### Leaf emergence

Leaves emerge when the growing degree days for soil temperature (0.05 m depth soil, third layer of CLM) since planting ( $GDD_{T_{soil}}$ , base 0 and 8 °C for C3 and C4 crop) reaches 3 % of  $GDD_{mat}$ . At this phase, available carbon is allocated to leaf, live stem, and fine root according to constant allocation coefficients. Leaf area index generally increases and reaches a maximum value, which is prescribed as  $6\text{m}^2\text{m}^{-2}$  for C3 and  $5\text{m}^2\text{m}^{-2}$  for C4 crop. Also, the stem area index is updated as stem carbon gain or loss.

$\beta_p$  is a plant functional type dependent variable that indicates the root water stress and varies from near zero (dry soil) to one (wet soil). We used  $\beta_p$  to better inform carbon allocation between root and shoot. When the soil is dry (small  $\beta_p$ ), more carbon is allocated to the root (Ericsson et al. 1996) to a maximum of 0.7. The rest of the available carbon is allocated to leaf and live stem in equal amounts.

### Grain fill to harvest

During the grain filling period, fine root carbon allocation is still controlled by  $\beta_p$ , while the maximum C allocation to fine root is changed to 0.2. 80 % of the remaining carbon is allocated to grain and the other 20 % to tissues that are not

explicitly simulated in the model, such as corn silk, flowers, etc. We assume the leaf and live stem carbon decline in this stage, and some portion of the carbon is transferred to grain

$$a_{froot} = 0.2(1 - \beta_p)$$

$$a_{leaf} = 0$$

$$a_{livestem} = 0$$

Covell S, Ellis RH, Roberts EH, Summerfield RJ (1986) The influence of temperature on seed-germination rate in grain legumes.

1. A comparison of chickpea, lentil, soybean and cowpea at constant temperatures. J Exp Bot 37:705–715

Daly C, Taylor G, Gibson W (1997) The PRISM approach to mapping precipitation and temperature. In: 10th conference on applied climatology, pp 10–12

De Ridder K, Gallee H (1998) Land surface-induced regional climate change in southern Israel. J Appl Meteorol 37:1470–1485

DeAngelis A, Dominguez F, Fan Y, Robock A, Kustu MD, Robinson D (2010) Evidence of enhanced precipitation due to irrigation over the great plains of the United States. J Geophys Res Atmos

$tran = c_{timestep}$

$\frac{GDD_{plant}}{GDD_p}$

doi:10.1029/2010JD013892

Di Luzio M, Johnson GL, Daly C, Eischeid JK, Arnold JG (2008)

Constructing retrospective gridded daily precipitation and temperature where  $tran$  is the transfer coefficient of leaf and live stem carbon to grain carbon,  $c_{timestep}$  is an adjusted coefficient for each timestep,  $GDD_{plant}$  is the soil growing degree days since planting (base 8 °C for C3 crop and 10 °C for C4 crop), and  $GDD_p$  is the 5-year running averaged soil growing degree days from April to September (base 8 °C for C3 crop and 10 °C for C4 crop).

## References

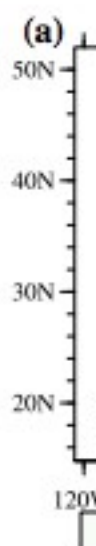
- Adams RM et al (1990) Global climate change and United-States agriculture. Nature 345:219–224
- Adegoke JO, Pielke RA, Eastman J, Mahmood R, Hubbard KG (2003) Impact of irrigation on midsummer surface fluxes and temperature under dry synoptic conditions: a regional atmospheric model study of the US high plains. Mon Weather Rev 131:556–564
- Adegoke JO, Pielke R, Carleton AM (2007) Observational and modeling studies of the impacts of agriculture-related land use change on planetary boundary layer processes in the central US. Agric For Meteorol 142:203–215

- Bonan GB (2008) Forests and climate change: forcings, feedbacks, and the climate benefits of forests. *Science* 320:1444–1449
- Bonhomme R (2000) Bases and limits to using ‘degree day’ units. *Eur J Agron* 13:1–10
- Boucher O, Myhre G, Myhre A (2004) Direct human influence of irrigation on atmospheric water vapour and climate. *Clim Dyn* 22:597–603
- Brown RA, Rosenberg NJ (1999) Climate change impacts on the potential productivity of corn and winter wheat in their primary United States growing regions. *Clim Chang* 41:73–107
- Butterfield RE, Morison JIL (1992) Modeling the impact of climatic warming on winter cereal development. *Agric For Meteorol* 62:241–261
- Collatz GJ, Ball JT, Grivet C, Berry JA (1991) Physiological and environmental-regulation of stomatal conductance, photosynthesis and transpiration—a model that includes a laminar boundary-layer. *Agric For Meteorol* 54:107–136
- Collatz GJ, Ribas-Carbo M, Berry JA (1992) Coupled photosynthesis-stomatal conductance model for leaves of C4 Plants. *Aust J Plant Physiol* 19:519–538
- Collins W et al (2004) Description of the NCAR Community Atmosphere Model (CAM 3.0) NCAR/TN-464+STR. National Center for Atmospheric Research, Boulder, Colorado, 226 pp
- Cook BI, Puma MJ, Krakauer NY (2011) Irrigation induced surface cooling in the context of modern and increased greenhouse gas forcing. *Clim Dyn* 37:1587–1600
- SPACeperature datasets for the conterminous United States. *J Appl Meteorol Clim* 47:475–497
- Easterling WE, Rosenberg NJ, Mckenney MS, Jones CA, Dyke PT, Williams JR (1992) Preparing the erosion productivity impact calculator (EPIC) model to simulate crop response to climate change and the direct effects of CO<sub>2</sub>. *Agric For Meteorol* 59:17–34
- Ericsson T, Rytter L, Vapaavuori E (1996) Physiology of carbon allocation in trees. *Biomass Bioenergy* 11:115–127
- Fang JY, Piao SL, Tang ZY, Peng CH, Wei J (2001) Interannual variability in net primary production and precipitation. *Science* 293:U1–U2
- Farquhar GD, Caemmerer SV, Berry JA (1980) A biochemical-model of photosynthetic CO<sub>2</sub> assimilation in leaves of C-3 species. *Planta* 149:78–90
- Feddema JJ, Oleson KW, Bonan GB, Mearns LO, Buja LE, Meehl GA, Washington WM (2005) The importance of land-cover change in simulating future climates. *Science* 310:1674–1678
- Fischer ML (2005) Carbon dioxide flux measurement systems. Handbook ARM TR-048, Atmospheric Radiation Measurement Climate Research Facility, U.S. Department of Energy
- Foley JA et al (2005) Global consequences of land use. *Science* 309:570–574
- Grell GA, Devenyi D (2002) A generalized approach to parameterizing convection combining ensemble and data assimilation techniques. *Geophys Res Lett* 29(14):1693. doi:[10.1029/2002GL015311](https://doi.org/10.1029/2002GL015311)
- Harding KJ, Snyder PK (2012a) Modeling the atmospheric response to irrigation in the great plains. Part II: the precipitation of irrigated water and changes in precipitation recycling. *J Hydrometeorol* 13:1687–1703
- Harding KJ, Snyder PK (2012b) Modeling the atmospheric response to irrigation in the great plains. Part I: general impacts on precipitation and the energy budget. *J Hydrometeorol* 13:1667–1686
- Higgins RW, Yao Y, Yarosh ES, Janowiak JE, Mo KC (1997) Influence of the Great Plains low-level jet on summertime precipitation and moisture transport over the central United States. *J Clim* 10:481–507
- Howell TA, Hatfield JL, Yamada H, Davis KR (1984) Evaluation of cotton canopy temperature to detect crop water-stress. *Trans ASAE* 27:84–88
- Jin JM, Miller NL (2011) Regional simulations to quantify land use change and irrigation impacts on hydroclimate in the California Central Valley. *Theor Appl Climatol* 104:429–442
- Jin JM, Miller NL, Schlegel N (2010) Sensitivity study of four land surface schemes in the WRF model. *Adv Meteorol* 2010:167436. doi:[10.1155/2010/167436](https://doi.org/10.1155/2010/167436)
- Kanamitsu M, Ebisuzaki W, Woollen J, Yang SK, Hnilo JJ, Fiorino M, Potter GL (2002) NCEP-DOE AMIP-II reanalysis (R-2). *Bull Am Meteorol Soc* 83:1631–1643
- space3362
- Y. Lu et al.
- spaceKenny JF, Barber NL, Hutson SS, Linsey KS, Lovelace JK, Maupin MA (2005) Estimated use of water in the United States in 2005. U.S. Geological Survey Circular 1344, p 52
- Kucharik CJ (2003) Evaluation of a process-based agro-ecosystem model (AgroIBIS) across the US corn belt: simulations of the interannual variability in maize yield. *Earth Interact* 7:1–33
- Kueppers LM, Snyder MA (2012) Influence of irrigated agriculture on diurnal surface energy and water fluxes, surface climate, and atmospheric circulation in California. *Clim Dyn* 38:1017–1029
- Kueppers LM, Snyder MA, Sloan LC (2007) Irrigation cooling effect: Regional climate forcing by land-use change. *Geophys Res Lett* 34:L03703. doi:[10.1029/2006gl028679](https://doi.org/10.1029/2006gl028679)
- Lascano RJ, Vanbavel CHM, Hatfield JL, Upchurch DR (1987) Energy and water-balance of a sparse crop—simulated and measured soil and crop evaporation. *Soil Sci Soc Am J* 51:1113–1121
- Lawlor DW, Mitchell RAC (1991) The Effects of increasing CO<sub>2</sub> on crop photosynthesis and productivity—a review of field studies. *Plant Cell Environ* 14:807–818
- Lawrence DM et al (2012) The CCSM4 land simulation, 1850–2005: assessment of surface climate and new capabilities. *J Clim* 25:2240–2260
- Levis S, Bonan GB, Kluzek E, Thornton PE, Jones A, Sacks WJ, Kucharik CJ (2012) Interactive Crop management in the Community Earth System Model (CESM1): seasonal influences on land-atmosphere fluxes. *J Clim* 25:4839–4859
- Li L, Li W, Jin J (2014) Contribution of the North Atlantic subtropical high to regional climate model (RCM) skill in simulating south-eastern United States summer precipitation. *Clim Dyn* 1–15. doi:[10.1007/s00382-014-2352-9](https://doi.org/10.1007/s00382-014-2352-9)
- Liang XZ, Xu M, Gao W, Reddy KR, Kunkel K, Schmoldt DL, Samel AN (2012) A distributed cotton growth model developed from GOSSYM and its parameter determination. *Agron J* 104:661–674
- Lo MH, Famiglietti JS (2013) Irrigation in California’s Central Valley strengthens the southwestern US water cycle. *Geophys Res Lett* 40:301–306
- Lobell DB, Field CB (2007) Global scale climate—crop yield relationships and the impacts of recent warming. *Environ Res Lett* 2:014002. doi:[10.1088/1748-9326/2/1/014002](https://doi.org/10.1088/1748-9326/2/1/014002)
- Lobell DB, Burke MB, Tebaldi C, Mastrandrea MD, Falcon WP, Naylor RL (2008) Prioritizing climate change adaptation needs for food security in 2030. *Science* 319:607–610
- Lobell D, Bala G, Mirin A, Phillips T, Maxwell R, Rotman D (2009) Regional differences in the influence of irrigation on climate. *J Clim* 22:2248–2255
- Lobell DB, Roberts MJ, Schlenker W, Braun N, Little BB, Rejesus RM, Hammer GL (2014) Greater sensitivity to drought accompanies maize yield increase in the US Midwest. *Science* 344:516–519
- Long SP, Ainsworth EA, Leakey ADB, Nosberger J, Ort DR (2006) Food for thought: lower-than-expected crop yield stimulation with rising CO<sub>2</sub> concentrations. *Science* 312:1918–1921
- Lu YQ, Kueppers LM (2012) Surface energy partitioning over four dominant vegetation types across the United States in a coupled regional climate model (Weather Research and Forecasting Model 3-Community Land Model 3.5). *J Geophys Res Atmos* 117:D06111. doi:[10.1029/2011jd016991](https://doi.org/10.1029/2011jd016991)
- Lu LX, Pielke RA, Liston GE, Parton WJ, Ojima D, Hartman M (2001) Implementation of a two-way interactive atmospheric and ecological model and its application to the central United States. *J Clim* 14:900–919

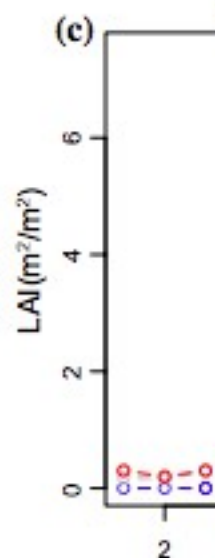
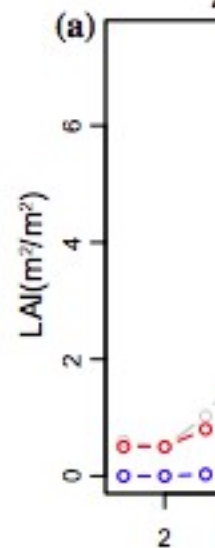


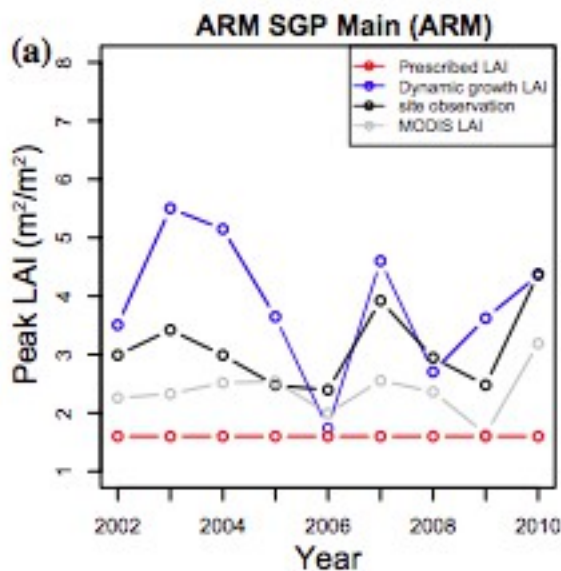
- Mearns LO, Rosenzweig C, Goldberg R (1992) Effect of changes in interannual climatic variability on CERES-wheat yields—sensitivity and  $\times\text{CO}_2$  general-circulation model studies. *Agr Forest Meteorol* 62:159–189
- Mendelsohn R, Nordhaus WD, Shaw D (1994) The impact of global warming on agriculture—a Ricardian analysis. *Am Econ Rev* 84:753–771
- spaceNakanishi M, Niino H (2006) An improved Mellor–Yamada level-3 model: its numerical stability and application to a regional prediction of advection fog. *Bound Layer Meteorol* 119:397–407
- Nielsen RL (2011) Field drydown of mature corn grain. Purdue University, West Lafayette, IN
- Oleson KW, Bonan GB, Levis S, Vertenstein M (2004) Effects of land use change on North American climate: impact of surface data-sets and model biogeophysics. *Clim Dyn* 23:117–132
- Oleson KW et al (2010) Technical description of version 4.0 of the Community Land Model (CLM). ISSN electronic edition 2153–2400, National Center for Atmospheric Research, Boulder, Colorado
- Osborne TM, Lawrence DM, Challinor AJ, Slingo JM, Wheeler TR (2007) Development and assessment of a coupled crop-climate model. *Glob Chang Biol* 13:169–183
- Osborne T, Slingo J, Lawrence D, Wheeler T (2009) Examining the interaction of growing crops with local climate using a coupled crop-climate model. *J Clim* 22:1393–1411
- Ottermann J (1977) Anthropogenic impact on albedo of earth. *Clim Chang* 1:137–155
- Ozdogan M, Salvucci GD (2004) Irrigation-induced changes in potential evapotranspiration in southeastern Turkey: test and application of Bouchet’s complementary hypothesis. *Water Resour Res* 40:W04301. doi:[10.1029/2003wr002822](https://doi.org/10.1029/2003wr002822)
- Peiris TSG, Thattil RO, Mahindapala R (1995) An analysis of the effect of climate and weather on coconut (*Cocos nucifera*). *Exp Agric* 31:451–460
- Pessaraki M (1999) Handbook of plant and crop stress. Marcel Dekker, New York
- Pitman A, Pielke R, Avissar R, Claussen M, Gash J, Dolman H (1999) The role of the land surface in weather and climate: does the land surface matter? *Int Geosph Biosph Program News Lett* 39:4–11
- Porter JR, Semenov MA (2005) Crop responses to climatic variation. *Philos Trans R Soc B* 360:2021–2035
- Rosenzweig C, Parry ML (1994) Potential impact of climate-change on world food-supply. *Nature* 367:133–138
- Sacks WJ, Cook BI, Buening N, Levis S, Helkowski JH (2009) Effects of global irrigation on the near-surface climate. *Clim Dyn* 33:159–175
- Sacks WJ, Deryng D, Foley JA, Ramankutty N (2010) Crop planting dates: an analysis of global patterns. *Glob Ecol Biogeogr* 19:607–620
- Saeed F, Hagemann S, Jacob D (2009) Impact of irrigation on the South Asian summer monsoon. *Geophys Res Lett* 36:L20711. doi:[10.1029/2009gl040625](https://doi.org/10.1029/2009gl040625)
- Sampaio G, Nobre C, Costa MH, Satyamurty P, Soares BS, Cardoso M (2007) Regional climate change over eastern Amazonia caused by pasture and soybean cropland expansion. *Geophys Res Lett* 34:L17709. doi:[10.1029/2007gl030612](https://doi.org/10.1029/2007gl030612)
- Siebert S, Doll P, Hoogeveen J, Faures JM, Frenken K, Feick S (2005) Development and validation of the global map of irrigation areas. *Hydrol Earth Syst Sci* 9:535–547
- Sorooshian S, Li JL, Hsu KL, Gao XG (2011) How significant is the impact of irrigation on the local hydroclimate in California’s Central Valley? Comparison of model results with ground and remote-sensing data. *J Geophys Res Atmos* 116. doi:[10.1029/2010jd014775](https://doi.org/10.1029/2010jd014775)
- Subin ZM, Riley WJ, Jin J, Christianson DS, Torn MS, Kueppers LM (2011) Ecosystem feedbacks to climate change in California: development, testing, and analysis using a coupled regional atmosphere and land surface model (WRF3-CLM3.5). *Earth Interact* 15. doi:[10.1175/2010ei331.1](https://doi.org/10.1175/2010ei331.1)
- Thompson G, Rasmussen RM, Manning K (2004) Explicit forecasts of winter precipitation using an improved bulk microphysics scheme. Part I: description and sensitivity analysis. *Mon Weather Rev* 132:519–542
- spaceCrop growth and irrigation  
3363
- spaceTsvetsinskaya EA, Mearns LO, Easterling WE (2001) Investigating the effect of seasonal plant growth and development in three-dimensional atmospheric simulations. Part II: atmospheric response to crop growth and development. *J Clim* 14:711–729
- Wagenvoort WA, Bierhuizen JF (1977) Some aspects of seed-germination in vegetables. 2. Effect of temperature-fluctuation, depth of sowing, seed size and cultivar, on heat sum and minimum temperature for germination. *Sci Hortic* 6:259–270
- Wanjura DE, Upchurch DR, Mahan JR (1992) Automated irrigation based on threshold canopy temperature. *Trans ASAE* 35:1411–1417
- Weaver SJ, Schubert S, Wang H (2009) Warm season variations in the low-level circulation and precipitation over the central United States in observations, AMIP simulations, and idealized SST experiments. *J Clim* 22:5401–5420
- spaceWise RR, Olson AJ, Schrader SM, Sharkey TD (2004) Electron transport is the functional limitation of photosynthesis in field-grown Pima cotton plants at high temperature. *Plant Cell Environ* 27:717–724
- Xu M, Liang X-Z, Gao W, Reddy KR, Slusser J, Kunkel K (2005) Preliminary results of the coupled CWRP-GOSYM system. *Remote Sens Model Ecosyst Sustain* II 5884. doi:[10.1117/12.621017](https://doi.org/10.1117/12.621017)
- Zeng XB (2001) Global vegetation root distribution for land modeling. *J Hydrometeorol* 2:525–530
- Zhu Z et al (2012) Global data sets of vegetation LAI3g and FPAR3g derived from GIMMS NDVI3g for the period 1981 to 2011. *Remote Sens* 4. doi:[10.3390/rs40x000x](https://doi.org/10.3390/rs40x000x)

**Fig. 1** Modeled domain showing **a** percent of cropland equipped for irrigation (%) within each grid cell (Siebert et al. 2005), and **b** mean 2004–2006 irrigation water applied (million gallons per day) simulated in WRF3.3-CLM4crop. The four AmeriFlux observational sites are indicated in **a**, Ne3 has the same location as Ne1



**Fig. 2** Simulated monthly LAI compared to observations at four AmeriFlux sites. Modeled and MODIS LAI are averaged for 2002–2011, and observed LAI is averaged for 2002–2010 for ARM SGP main site, 2002–2007 for Mead irrigated and rainfed sites, and 1997–2001 for Bondville)





**(a)** Fig. 5 Comparison of simulated and observed soil moisture. **a** Soil water (0–0.5 m) difference between CROP and observed and **b** soil moisture comparison at the Mead irrigated site

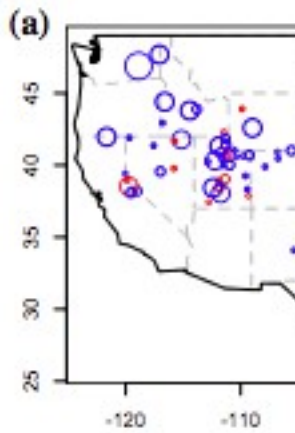


**Fig. 3** Variation in simulated annual peak LAI comp

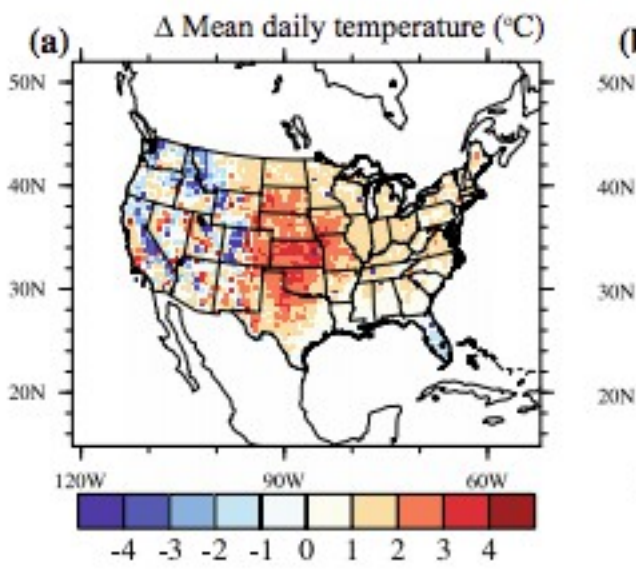


**Fig. 4** Averaged (2004–2006) difference between th temperature, and c precipitation

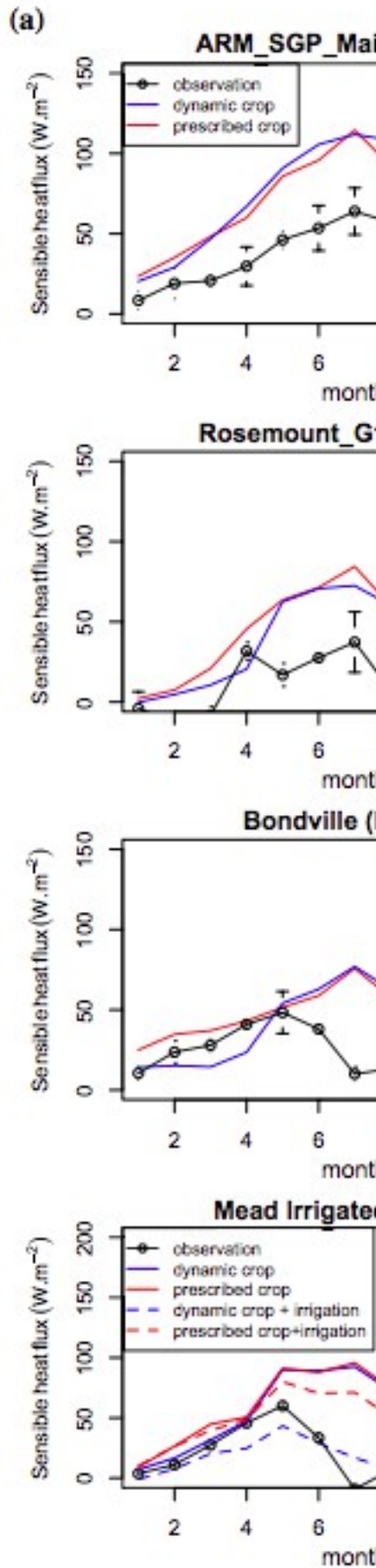


**Fig. 7** Monthly variation in domain averaged **a** irrigation water (mm/day) and **b** leaf area index ( $m^2/m^2$ ) in prescribed crop and dynamic crop simulations

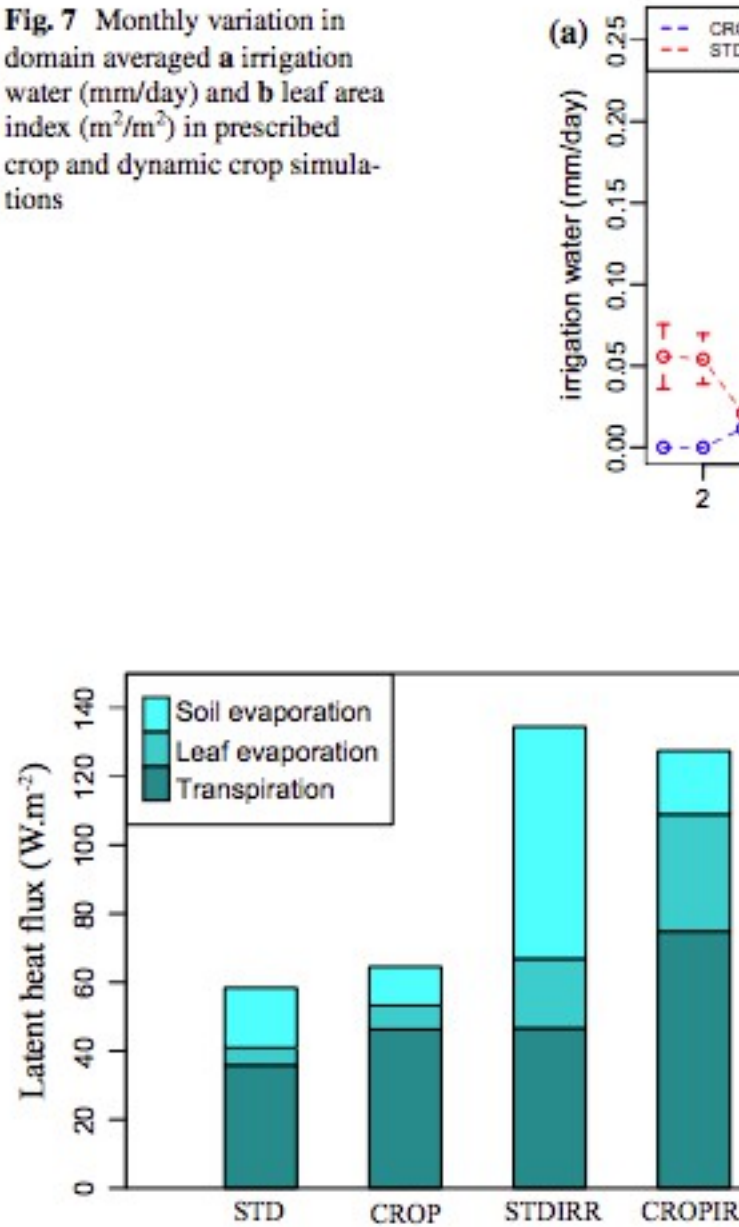


**Fig. 8** Simulated 2004–2006 averaged latent heat flux partitioned into three components for the four models

**Fig. 9** 2004–2006 JJA averaged difference along different grid cell irrigated cropland percentage of **a** latent heat flux ( $\text{W m}^{-2}$ ), **b** sensible heat flux ( $\text{W m}^{-2}$ ), **c** net radiation ( $\text{W m}^{-2}$ ), **d** 2 m air temperature ( $^{\circ}\text{C}$ ), **e** soil moisture ( $\text{m}^3 \text{m}^{-3}$ ), and **f** Bowen ratio reduction (%) in prescribed crop and dynamic crop simulations. The *error bar* shows the standard error among 9 months

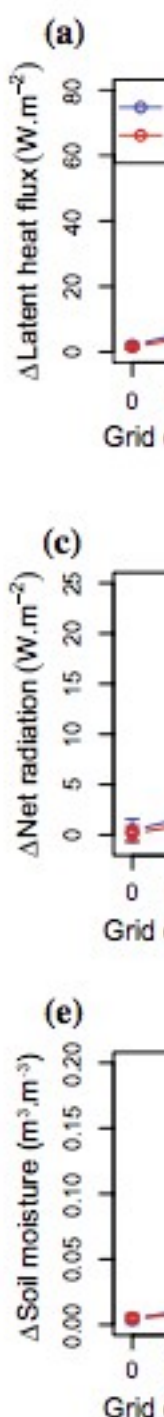


**Fig. 10** Monthly variation of 2-m air temperature for the eight 1-year offline simulations and site observation

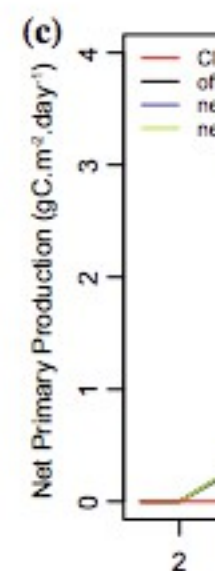
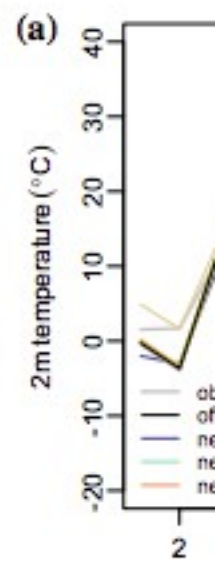
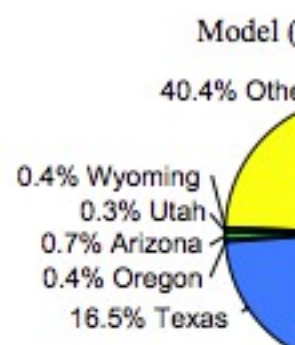


**Fig. 11** State level irrigation percentages for model (CROPIRR) and USGS in 2005. The total amount applied is 143 million gallons per day in CROPIRR, and 128 million gallons per day according to the USGS survey





occurs when the crop reaches 1.5 times the for maturity rather than occurring as soon as reaches maturity as in CLM4CNCrop, since crops such as corn (Nielsen 2011) are left in the field until maturity to dry. We also modified the carbon allocation to reflect environmental stress on crop growth section A3 of the appendix.

## Phenology

### Planting

The thresholds for planting, and thus initiating the development cycle, are defined as:

$$T_{2m} > T_p$$

$$GDD_8 > GDD_{min}$$

where  $T_{2m}$  is the instantaneous 2-m air temperature,  $T_p$  is a crop-specific planting temperature (7 °C for C3 crop and 10 °C for C4 crop),  $GDD_8$  is the 5-year running averaged growing degree days (base 8 °C) from March to September, and  $GDD_{min}$  is the minimum growing degree days requirement (50 degree days for both C3 and C4 crop). C3 crop must meet the planting temperature between March 1st and May 14th, and C4 crop must meet the planting temperature between May 1st and June 14th.

At planting, some initial values are assigned: leaf area index (0.1 m<sup>2</sup>/m<sup>2</sup>), stem area index (0.1 m<sup>2</sup>/m<sup>2</sup>), leaf carbon (3 gC/m<sup>2</sup>), stem carbon (3 gC/m<sup>2</sup>), and root carbon (4.5 gC/m<sup>2</sup>). The growing degree days necessary for the crop to reach vegetative and reproductive maturity,  $GDD_{mat}$ , is updated:

$$GDD_{mat}^{C3crop} = 0.85GDD_8$$

$$GDD_{mat}^{C4crop} = 0.85GDD_{10}$$

$$GDD_8 = GDD_8 + T_{2m} - 8, \quad 0 \leq T_{2m} - 8 \leq 8$$

$$GDD_{10} = GDD_{10} + T_{2m} - 10, \quad 0 \leq T_{2m} - 10 \leq 10$$

where  $GDD_8$  and  $GDD_{10}$  are the 5-year running averaged growing degree days from March to September

explicitly simulated in the model, such as corn silks, grain, etc. We assume the leaf and live stem carbon dynamics are not explicitly simulated at this stage, and some portion of the carbon is transferred to grain

$$a_{root} = 0.2(1 - \beta_p)$$

$$a_{grain} = 0.8(1 - a_{root})$$

$$a_{leaf} = 0$$

$$a_{livestem} = 0$$

$$tran = c_{timestep} \left( \tan \frac{GDD_{plant}}{GDD_p} \right)$$

where  $tran$  is the transfer coefficient of leaf and live stem carbon to grain carbon,  $c_{timestep}$  is an adjusted coefficient for each timestep,  $GDD_{plant}$  is the soil growing degree days since planting (base 8 °C for C3 crop and 10 °C for C4 crop), and  $GDD_p$  is the 5-year running averaged soil growing degree days from April to September (base 8 °C for C3 crop and 10 °C for C4 crop).